EXPERIMENTAL AND NUMERICAL ASSESSMENT OF HELICOPTER SUBFLOOR CRASHWORTHINESS

Marco ANGHILERI
Associate Professor *
marco.anghileri@polimi.it

Andrea MILANESE
Graduated Laboratory Technician *
andrea.milanese@polimi.it

Angelo SURINI*
Graduated Engineer *
angelo.surini@polimi.it

* Politecnico di Milano, Department of Aerospace Engineering, Via La Masa 34, 20156, Milan, Italy

Keywords: *Helicopter subfloor, Crashworthiness, Experimental Tests, Nonlinear Finite Element Analysis*

ABSTRACT

A research project aimed at improving the conceptual design of helicopter subfloor with regard to structural and crash requirements was started at LaST Crash Labs in cooperation with AgustaWestland. The research consisted both of experimental and numerical activities. The subfloor is usually made of light aluminum alloy and absorbs the impact energy through plastic deformation. Experimental tests were carried out at different levels. Initially, drop tests were carried out to investigate the crash absorption capabilities of various intersection designs. The intersection between spars and frames is that part of the helicopter subfloor that gives the greatest contribution to the impact energy absorption during a crash landing. Subsequently, a whole section of the subfloor was crash tested using a horizontal impact sled facility. Finally, a full scale drop test was carried out with the entire subfloor, a seat and anthropomorphic test device (ATD). In parallel, numerical activity were carried out using LS-DYNA – a commercially available nonlinear finite element code, widely diffuse for crash. A robust numerical model of the intersections was initially created and validated against the first test results. The validated model was then used to support the development of the intersection design and to obtain useful indications to prepare the test on the full subfloor. A numerical model of the full scale test was eventually created and the results compared with the data collected during the test referring to the most relevant correlation indexes in terms of absorbed energy. As a result, although the numerical model fail to capture the entire event (due to the complexity of the event itself) the correlation parameters considered showed that it provided an acceptable representation of the event in terms of energy absorption, crash efficiency and collapse mode and therefore it can be used to support and guide further development of the subfloor. This article presents the work related to the tests on individual intersections and four walled cells of the subfloor.

INTRODUCTION

To improve the conceptual design of a helicopter, able to fulfill both the structural and impact resistance requirements, a research program to study the energy absorption capacity of the subfloor was started. In particular crash tests have been performed on the structure of the subfloor and on the intersection elements, being the parts of the structure that can introduce a high peak of deceleration at the floor of the cabin causing harm to the occupants. Beside the above mentioned requirements, the design of a helicopter should prevent risk of fire, cockpit collapse as well as the collision between the occupants and the furniture. This is commonly obtained through the use of energy-absorbing elements incorporated in the landing gear, the subfloor and in the seats [2]. The structure of the subfloor must thus be designed to limit, through structural deformation, the deceleration of the cockpit. Particular attention should be given to the design of the intersections between the beams and bulkheads, which makes an essential contribution to the crash behavior of the subfloor [5].Commonly the subfloor is made of light aluminum alloy and absorbs the impact energy through plastic deformation. The research and studies that have taken place are oriented in three directions:

- the study of materials used to absorb energy: in the past only light metal alloys were used while today honeycomb, foam and especially fiber-based composites are adopted [9-11-13], to combine a high energy absorption capacity with relatively low weights;

- the study and optimization of new high-efficiency geometries [3-4-7-8-10]. To control the buckling phenomenon and prevent the total loss of post-crash resistance two solutions were studied: the first is to reinforce the panel with other materials such as foam, honeycomb, while the second is to model the panel so that it has a non-planar geometry;

- the correlation between the results of experimental tests [1-6] and numerical analysis to reduce development cost and to enable numerical optimization of the design.

This article gives special coverage to the latter, aiming to obtain a robust and efficient model that can be used in the future to reduce the number of trials needed in the design and validation phase.

1 EXPERIMENTAL TESTS

1.1 Test on a single intersection

Twelve dynamic compression tests were performed on four types of intersection with different thickness, rivet size and stiffener cross section type (T and J). The specimen was crushed on a vertical drop-test setup with a rail driven mass of 110 [kg] hitting the structures at a velocity of 8.4 [m/s]. During the tests the acceleration was measured by two piezoresistive accelerometers placed on the impacting mass. Data acquisition system consisted of a 16 channels Pacific Instrumentation with programmable gain, power and sample rate up to 100 [kHz] per channel. Data were filtered through a digital filter type SAE CFC 180. Tests were also captured through a high-speed camera Photomark V5.1 with up to 100 [kfps]. The displacement was obtained through double numerical integration while the force was recovered from the mass-acceleration product. These results where then plotted to obtain the required force – displacement curve. The work presented here refers to the testing of the type-J stiffener specimens.

For each experimental test different parameters [3] were calculated. These parameters are able to fully characterize strength, absorption and efficiency of the tested specimen.

Fig. 1 - Intersection cruciform element before test

Fig. 2 - Intersection cruciform element after test

These parameters provide valuable information on the overall design quality of the absorber and are of critical importance to assess an all-round correlation with numerical models, thus improving the common force-displacement correlation. Besides the classical parameters of absorbed energy and mean force, obtained as the ratio of energy absorption and crushing distance, other meaningful quantities were computed like the distance of maximum efficiency (d max), over which the strength is too high compared to the first peak. The ratio between d max and the initial length d0 is a spatial efficiency index called "stroke efficiency" Se. All parameters were also computed at a common distance s to establish an estimate of the numerical-experimental correlation at a given point on the force-displacement curve.

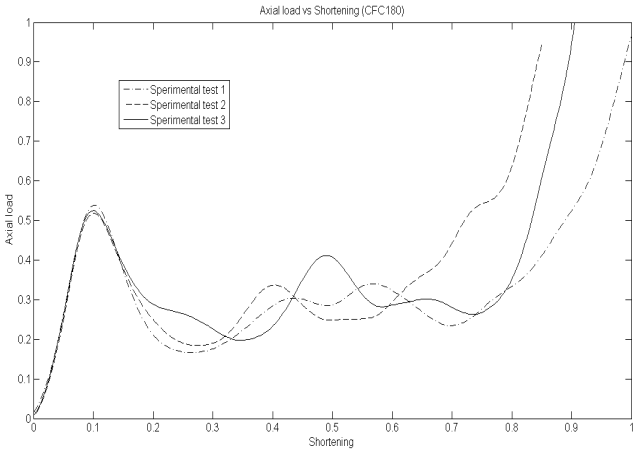

Fig. 3- Intersection cruciform element: experimental curve Axial load vs Shortening

The Table 1 shows the energy and force rating relative to a crushing length of s and d max , as well as the two highest force peaks before complete crush:

	d_{max}	s	$E(d_{max})$	E(s)	Se
Sper1	0.907	0.803	0.267	0.223	0.565
Sper2	0.770	0.803	0.239	0.257	0.482
Sper3	0.835	0.803	0.254	0.239	0.522

	$Favg(d_{max})$	Favg(s)	F(pk1)	F(pk2)
Sper1	0.295	0.278	0.539	0.341
Sper2	0.310	0.320	0.519	0.337
Sper3	0.304	0.298	0.525	0.412

Table 1– Experimental parameters

1.2 Subfloor cell experimental tests

Nine dynamic compression tests were then performed on three types of subfloor cell with different intersection, stiffeners and spar arrangement. The characterization tests were performed on a pneumatically driven horizontal sled of 640 [kg] mass at an impact velocity of 6 [m/s]. The specimen was tied to a rigid base, which was fixed perpendicularly to the lab floor. During the tests, the acceleration was measured by two piezoresistive accelerometers positioned at the center of the sled.

Fig. 4- Subfloor cell before test

The data acquisition system consisted of an IOTECH STRAINBOOK 616 with 8 input channels and a sample rate of 12500 [Hz] per channel. Data were filtered through a type SAE CFC 180 digital filter. Tests were captured through the same high-speed camera Photomark V5.1 with up to 100 [kfps]. Filtered acceleration data and impacting mass ware then used to recover the crush force vs. time graph, as required by AgustaWestland.

Fig. 5- Subfloor cell after test

Our work focuses on the cell with the J-type stiffener for further numerical and experimental comparison. As stated above the accelerometer was placed on the sled. The measurement data, filtered with the SAE CFC 180, still contains part of the structural vibrations of the sled. Choosing a more conservative filter like a CFC 60 produced a very smooth curve, but it also dampened the first peak.

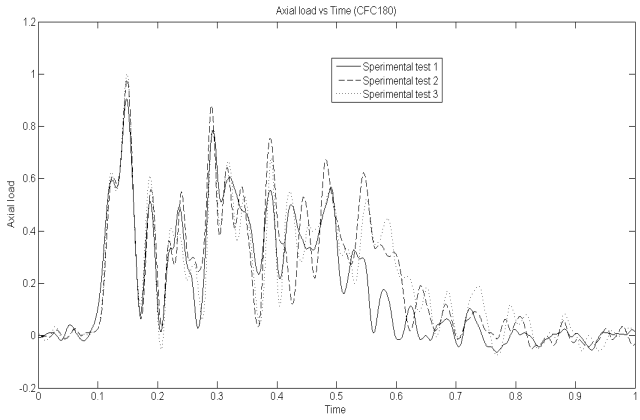

Fig. 6 - Subfloor cell: experimental curve Axial load vs Time

We decided to use the CFC180 filter to get a better evaluation of the first force peak while maintaining a fair estimation of the average value.

2. FINITE ELEMENTS MODELS

2.1 Numerical tests on single intersection model

The model used in the analysis of the intersection was obtained from the CAD and is therefore a faithful reproduction of the three intersections tested experimentally. The model is mainly composed of shell elements and beam elements. Since the beginning of the work rivets were considered key elements for the validation of the intersection's crash behavior and special attention was made on their modeling. Two node beam elements were favored over hexahedral ones as the high linear density made transmitted torque negligible. The rivets were modeled as point welds. Card *SECTION_BEAM was used to express chosen beam formulation and its cross section. Rivets material (Al 2117-T4) was implemented using the specialized Ls-Dyna's formulation (MAT-100). The rivets and the shell elements were connected by a CONTACT_SPOTWELD card as nodal connection would tie the mesh size to the number of rivets, thus limiting the use of the model in design optimization techniques. The evolution of the model has seen the change of many parameters that allowed us

to obtain the results shown in the graph in Fig. 8. At the beginning a series of tests were carried out to identify the correct numerical friction coefficients. Although the very first results of strength and energy were comparable, there was a remarkable difference between the deformation mode of the numerical model and the one of the experimental tests. In particular the spar and the stiffener separated after the failure of the rivets (which does not occur in tests). This has led to further analysis of the elastic and plastic behavior of rivets s which revealed the following possible causes of such a different behavior:

- un-modeled static friction between the plates due to the pre-compression prior to riveting. This pre-compression results in a transfer of tangential stresses effort in the area interested thus reducing the load on the joints;

- the excessive rigidity of the contact with the impacting mass.

To limit this phenomenon and thus prevent the failure of the topmost rivets the yield strength was selectively increased. A subsequent stress analysis revealed that the axial and cutting forces acting on the other rivets were considerably higher than the typical strength of the elements. This was leading to another earlier break in the upper part of the specimen and then a low correlation in the crushing mode of the column. To contain this problem a global mesh refinement was adopted, bringing the typical mesh size of the spars and diagonal walls from 3 [mm] to 1.5 [mm] (Fig.7). The increased computational cost is then balanced by a better stress distribution in the rivet area, which finally led to a satisfying correlation of the numerical model. A better correlation in the crushing mode was then finally achieved changing the main material model, from a simple and widely used piecewise elastic-plastic representation to a modern incremental-damage Johnson-Cook (JC) model.

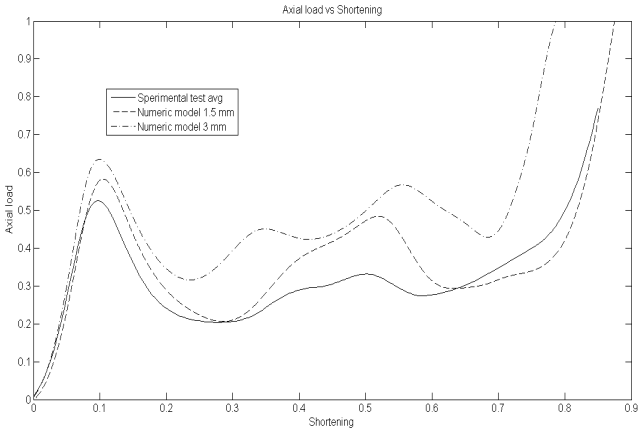

Fig. 7- Influence of the mesh size on FE simulations

The finite element solver used already implemented the JC model in the material library, so data from a recent experimental work was used [12] . For the reader's convenience the data is presented in Table 2.

Young's Modulus [MPa]	Poisson's Modulus	A [MPa]	B [MPa]	n	C
72000	0.313	265	426	0.34	0.015
m	D_1	D_2	D_3	D_4	D_5
1	0.13	0.13	-1.5	0.011	0

Table 2- Johnson-Cook model properties for 2024-T3 Aluminum Alloy

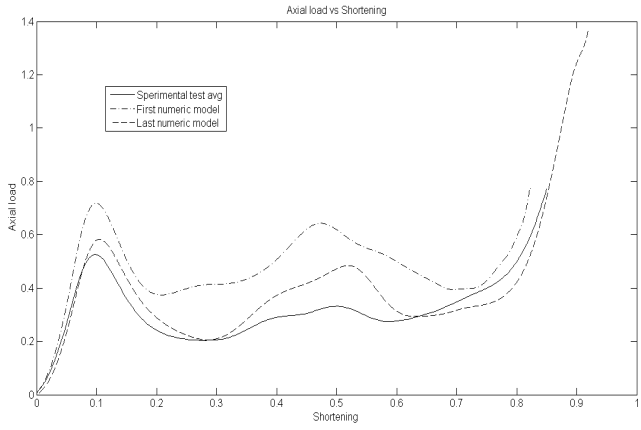

Fig. 8- Numerical and experimental load-shortening diagrams of the intersection cruciform element

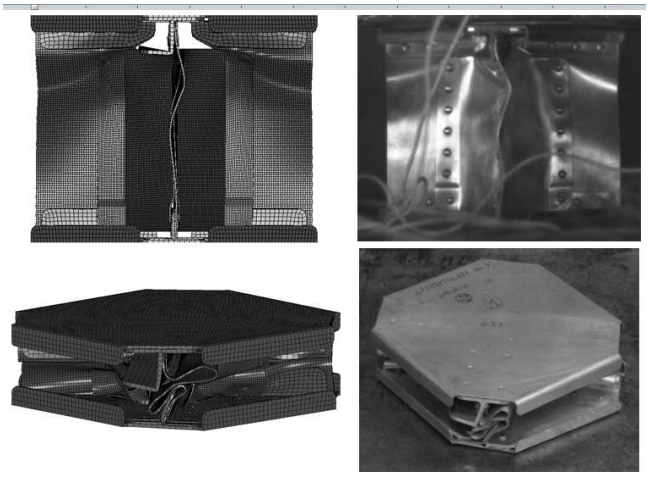

Fig. 9– Comparison between experimental and numerical deformations of the intersection cruciform element

For each test, numerical and experimental, several parameters were calculated to summarize the strength, absorption and efficiency behavior of the columns.

$$E(d) = \int_0^d F(x)dx \qquad (1)$$

$$F_{avg}(d) = \frac{E(d)}{d} \qquad (2)$$

$$A_E(d) = \frac{F_{avg}(d)}{F_{\max}(d)} \qquad (3)$$

$$T_E(d) = \frac{E(d)}{F_{\max}(d) \cdot l} \qquad (4)$$

These parameters, in addition to providing valuable information on the actual goodness of design of the absorber in its entirety, are of fundamental importance to assess a degree of correlation that does not stop at the, still extremely valuable, force-displacement curve. The following table presents the correlation indexes calculated: the correlation indices "r" and "corr" represent in turn the average error and the average correlation with the experimental evidence.

	corr_fo	corr_en	corr_F_{avg}	corr_A_E	corr_T_E
First numeric model	0.641	0.996	0.829	0.535	0.997
Last numeric model	0.780	0.997	0.918	0.730	0.993

	r[E(d_{max})]	r[E(s)]	r[Se]	r[Fpk1]	r[Fpk2]
First numeric model	0.467	0.418	0.940	0.638	0.215
Last numeric model	0.867	0.861	0.945	0.895	0.655

Table 3- Correlation parameters of the intersection element

As previously mentioned, despite an excellent energy correlation of the first models we chose to further refine the model to fix several deformation mode differences between the numerical model and the hi-speed video capture of the experimental tests. In particular, the failure of almost all of the rivets, the rotation of the specimen during crushing and overall incoherence of the deformation led us to investigate the causes and possible solutions to them. The decision to invest time in building a more satisfactory model has been rewarded by the identification of the main problems of the numerical model used initially.

2.2 Testing of the subfloor cell model

Development of the sub-floor cell numerical model took a minor amount of time thanks to the good correlation of the column model.

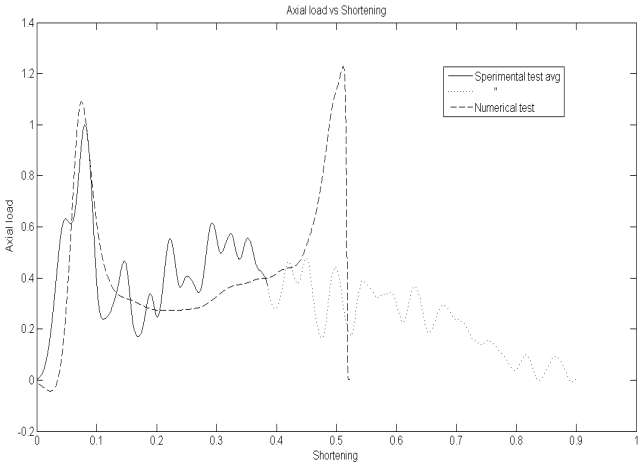

Fig. 10- Numerical and experimental load-shortening diagrams of the subfloor cell

As the same solutions developed for the single junction were adopted in the complete cell a good correlation in terms of average forces was immediately obtained. That can be seen as a good index of the robustness of the model previously developed. The curve obtained is shown in Fig. 10. The graph shows a good correlation in the initial phase of the test, while in middle of the crush length the numerical test managed to capture only the average force, probably due to the vibrations introduced by the impact in the experimental test. The mismatch of the final part can be considered acceptable because it is associated with low velocity and therefore energy absorption, although great care must be taken in making assumptions about the max crushing length of the cell. Two conclusions can be made from this evidence:

- at a preliminary project level one must consider the overestimation of the absorbed energy by the numerical model;

- at the certification phase the model is conservative due to the overestimation of the loads coming to the occupants, but its use could be problematic if absolute weight optimization is required.

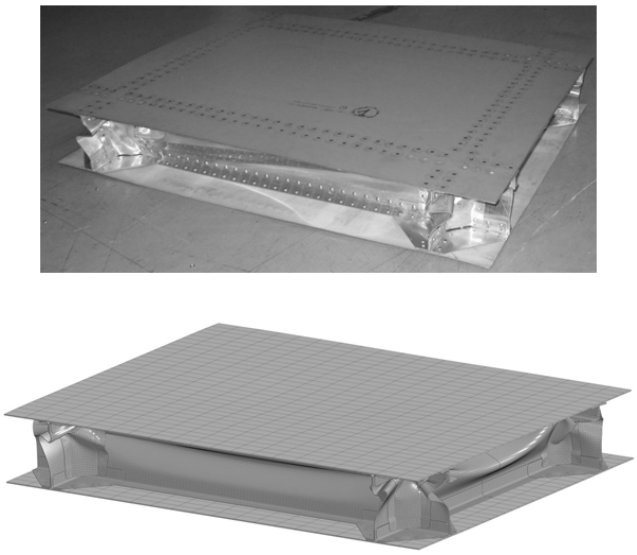

Fig. 11- Comparison between experimental and numerical deformations of the subfloor cell

3. CONCLUSIONS

The article presented the work done in collaboration with AgustaWestland on the study and development of a numerical model of a modern helicopter subfloor. In particular, the work focused on the optimization of correlation indexes between tests performed on individual intersections and complete four-walled cells of the subfloor. Three factors were identified as of critical importance for the robust implementation of such a model:

- an incremental damage material;

- the mesh size around the joints;

- the friction and viscous friction coefficients.

Although results on the complete cell are not completely correlated to those obtained experimentally we can be satisfied with the model developed for the intersection in that, as demonstrated by the correlation parameters used, it faithfully represents the evolution of energy absorption, crash efficiency and collapse mode. Good results have led us to implement this model for the simulation of a complete test which includes the sub-floor cell, a helicopter seat and an anthropomorphic crash test dummy. This test will be described in a later publication.

References

[1] Alguadich, S. (s.d.). Full scale crash test for cabin safety research. Italian aerospace research center - (CIRA) , 1-13.

[2] Bisagni, C. (2002). Crashworthiness of helicopter subfloor structures. International Journal of Impact Engineering , 1-16.

[3] Bisagni, C. (s.d.). Optimization of an helicopter subfloor under crash conditions. 1-16.

[4] Bisagni, C. (n.d.). Retrofit design of a crashworthy subfloor for a commuter aircraft. 1-13.

[5] Giavotto, V. (2000). The Significance of Crashworthiness. Proceedings of the CEAS FORUM on "Crash Questions", Capua, Italy , 1-11.

[6] K. Hughes, R. V. (2007). Experimental observations of an 8m/s drop test of a metallic helicopter underfloor structure onto a hard surface: part 1. Proceedings of the Institution of Mechanical Engineers, Part G: Journal of Aerospace Engineering - Vol 221, Number 5 , 661-678.

[7] L. Lanzi, A. A. (2006). Optimisation of energy absorbing subsystems for helicopter vertical crashes. 25th International Congress of the aeronautical sciences (ICAS) , 1-10.

[8] L. Lanzi, C. B. (2004). Crashworthiness optimization of helicopter subfloor based on decomposition and global approximation. Industrial applications , 401-410.

[9] L. Lanzi, C. M.-L. (2004). Crashworthiness shape optimization of helicopter subfloor intersection elements. 24th International Congress of the Aeronautical Sciences (ICAS) , 1-10.

[10] Lee, P. H. (1997). Topological optimization of rotorcraft subfloor structures for crashworthiness considerations. Computers and Structures Vol.64 , 65-76.

[11] M. A. McCarthy, J. F. (2001). Numerical investigation of a crash test of a composite helicopter subfloor structure. Composite Structures , 345-359.

[12] Research, O. o. (2000). Experimental investigation of material models for Ti-6Al-4V Titanium and 2024-T3 Aluminum. U.S. Department of Transportation , 17.

[13] S. T. Taher, E. M. (2006). A new composite energy absorbing system for aircraft and helicopter. Composite Structures , 14-23.

Copyright Statement